TELKOMNIKA Telecommunication, Computing, Electronics and Control
Vol. 18, No. 6, December 2020, pp. 3142~3154
ISSN: 1693-6930, accredited First Grade by Kemenristekdikti, Decree No: 21/E/KPT/2018
DOI: 10.12928/TELKOMNIKA.v18i6.14571

Comparative analysis of PID and neural network controllers for improving starting torque of wound rotor induction motor

Hashmia Sh. Dakheel[1], Zainab B. Abdulla[2], Helen Jasim Jawad[3], Ali Jasim Mohammed[4]
[1,2]Department of Electromechanical, University of Technology Baghdad, Iraq
[3]Department of Electrical, University of Technology Baghdad, Iraq
[4]Ministry of education/Directorate of vocational education, India

Article Info

Article history:

Received Nov 11, 2019
Revised Jun 21, 2020
Accepted Jul 9, 2020

Keywords:

External resistance (R_{ext})
NARMA-L2
PID controller
Starting torque (T_s)
Wound rotor induction motor

ABSTRACT

Unlike 3-phase squirrel cage induction motor, starting-up of 3-phase wound rotor counterpart can be improved by adding an external resistance to the rotor circuit. Thus, leads to reduce starting current and increase starting torque. In this paper two controllers for 3-phase wound rotor induction motor have been proposed include conventional proportional integral derivative (PID) controller and the other based on artificial neural network (NARMA-L2). A comparison between these controllers has been conducted. It has been shown that starting torque of the motor has been improved, when utilizing the neural network controller compared to the conventional counterpart. It should be noted that MATLAB/SIMULINK has been used to implement both controllers.

Corresponding Author:

Hashmina Sh. Dakheel,
Department of Electromechanical,
University of Technology,
168 Al-Sinna' street, 10066, Baghdad, Iraq.
Email: hashimia.shr@yahoo.com

1. INTRODUCTION

The induction motors (IM) are greater used than 60% of total electric strength consumed worldwide [1]. IM have unique advantages such as slow maintenance, high robustness, and low cost which makes it to be suitable for industrial applications [2-5]. Wound-rotor induction motor (WRIM) has some specified applications that requires a high torque, adjustable speed drives, high inertia loads, so in order to improve the performance of WRIM use several methods of rotor control which include resistance and impedance [1]. The rotor of IM has 3-phase winding connected in star, and slip rings are connected to the rotor winding, these rings give the possibility of connecting external resistance *(R_{ext})* adding to the rotor that helps in speed control of WRIM [6]. The authors of [7] present a new method for soft starting of IM in rotor circuit that represented in a parallel combination of resistors, self-inductors and capacitors to obtain soft and higher starting torque *(T_s)* and starting current is limited. In [8] this study presents different methods of starting performance for 3-phase wound-rotor IM that include variable rotor resistance, online direct and double feed starting as well as compare them, this study achieves high starting torque by using double feed starting. Study [9] refer to different starter connected with IM

which represented in auto-transformer starter, and direct-on-line at starting by using MATLAB SIMULINK to analysis starting current, torque and speed also compare them. This research used dynamic simulation of speed-control and starting for wound-rotor of IM based on differential equations for angular velocity and flux linkages [10] and comparison between developed model with experimental results in laboratory. In study [11] show using chopper control resistance and feedback circuit to obtain constant speed and constant torque, the speed for a given load torque may be varied by varying the rotor resistance. There are many types of controllers can be utilized with the motors such as proportional integral derivative (PID) controller, these controllers are widely used in industrial applications for control which have a reasonable performance and different plants.

Hence, the gain parameters of PID can be obtained by evolutionary algorithms [12]. Because of parameters and non-linear behavior of IM, the process of control convergence has many problems at different conditions of operating, thus chooses artificial intelligent controller (AIC) that represents the best one for IM control, the use of artificial neural networks (ANN) for nonlinear system modeling and control has demonstrated to be extremely successful because of their ability to learn the dynamics of the plant, robustness, inherent approximation capability and a high degree of tolerance [13]. With the development in artificial intelligence applications, neural network has been used in identification and control of linear and non-linear systems.

The main advantage of ANN based techniques over conventional techniques is non-algorithmic parallel-distributed architecture for information processing that allows it to learn any complex input-output mapping, ANN is extremely useful in the area of learning control and capability of learning by training data under diverse operations conditions [14], therefore this paper includes study the effect of adding R_{ext} to the rotor circuit of WRIM in order to improve T_s that is represented one of the most characteristics of IM at starting operation condition, as well as comparison between PID controller and ANN (NARMA-L2) at different values of these resistance in order to improve and obtain the maximum and best T_s to develop performance of WRIM.

2. STARTING TORQUE

The starting torque is one of great importance in case of driving high-inertia loads that is proportional to the rotor resistance. It's necessary to have an excessive resistance at some points of starting period, and reduce the value of this resistance until put off from rotor circuit while motor reaches to steady state case so that the starting current is usually limited in drivers in order to protect the winding from the over load current and low voltages at starting and breaking cases of the motor [7]. Therefore, it is required to a starter in the circuit of motor and reduced the applied voltage to the motor at starting condition [9].

3. STARTING WITH EXTERNAL RESISTANCE

In wound-rotor induction motor (WRIM) is additionally R_{ext} to the rotor circuit for the duration at starting as a result as shown in Figure 1 shows WRIM with rotor external resistance [15]. When T_s increase and rotor current decrease, that is very important to obtain a maximum torque (T_{max}) at starting condition, this resistance proportional to the slip, when the resistance value is high, the slip will be increase instantly, for that reason it is viable to attain "pull-out" torque even with low speeds [15, 16]. Whilst the motor reaches its rated speed as the R_{ext} is removed and when the motor operates at steady state condition, it behaves in the identical way as squirrel-cage induction motor [16]. The value of rotor resistance specifies the torque consequently; when the rotor resistance is increasing at a regular torque reasons a proportionate increase in the motor slip with lower in speed of rotor, because of that, the rate for a given load torque can be varied by various rotor resistance, its illustrates as show in (1) and to achieve high T_s, to obtain T_{max} at stand still should be chosen the value of R_2 is appropriately as shown in Figure 2 indicate to mechanical characteristic at variable values of R_{ext} [17].

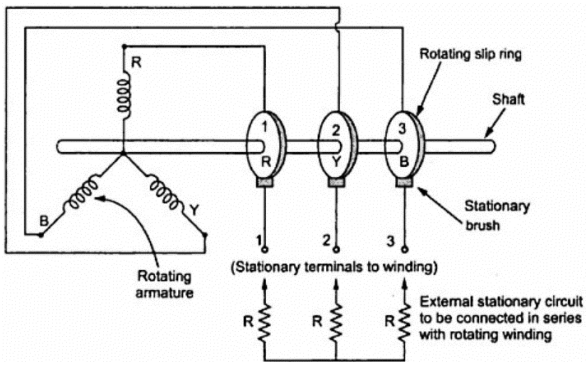

Figure 1. WRIM with external resistance

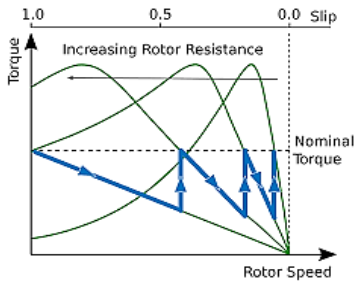

Figure 2. Mechanical characteristic of WRIM

$$T = \frac{K_S \, E_2^2 R_2}{R_2^2 + S^2 X_2^2} \quad (1)$$

4. PID CONTROLLER

PID controllers consist of 3 fundamental control modes, which are proportional, integral and derivative modes, these modes are extensively utilized in control system especially in industrial applications, they are simple to implement and provide good performance. The process of this controller includes set points and feedback to perform, as show in (2) refers to this process in domain time [18].

$$U(T) = K_p \, e(t) + K_i \int_0^t e(t)dt + K_d \frac{de(t)}{dt} \quad (2)$$

PID controller (proportional integral derivative controller) is widely used in industrial control system, it is calculates an "error" value as the difference between the measured process variable and the desired set point [19-21], a proportional controller may not give steady state error performance which is needed in the system, an integral controller may give steady state error performance, but it slows a system down. So, the addition of a derivative term helps to cure both of these problems, Figure 3 illustrates a basic block of PID controller [22-24]. Figure 4 shows simulink model of WRIM that is proposed in this work without any controllers, and Figure 5 refers to the model with PID controller and subsystem include the simulink model of WRIM.

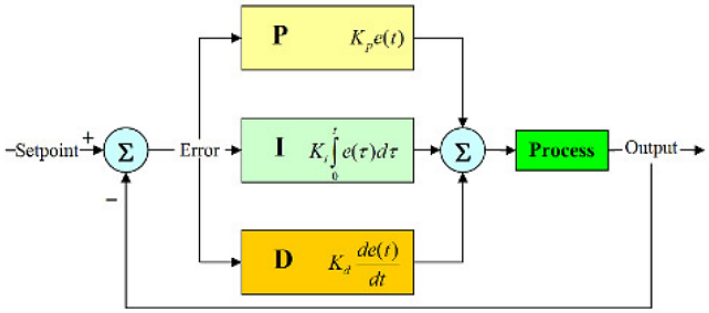

Figure 3. Basic block of PID controller

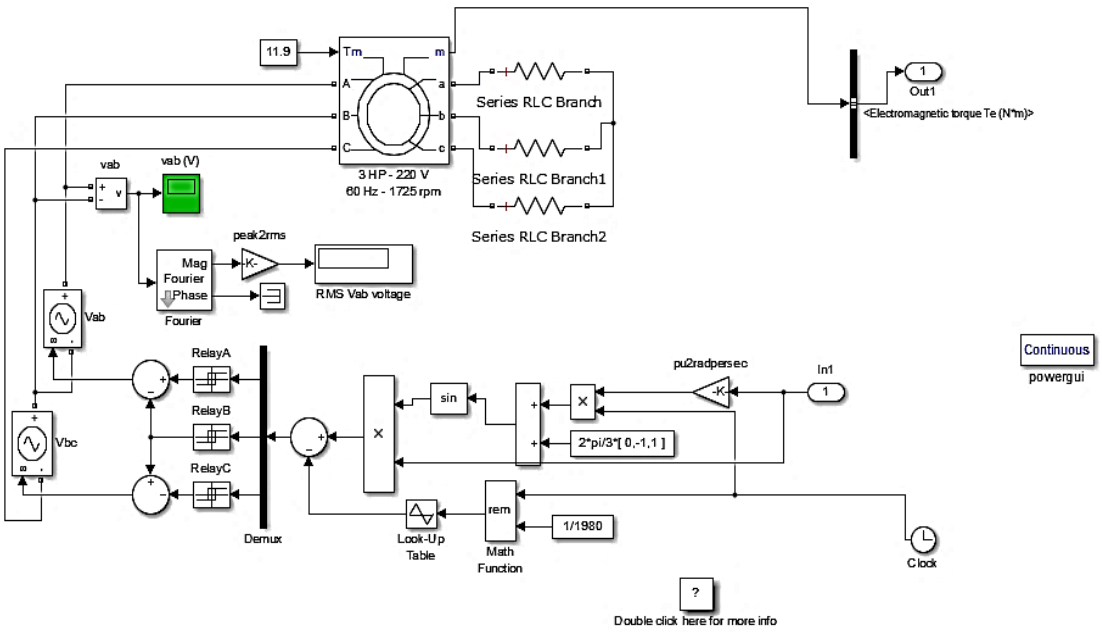

Figure 4. Simulink model of WRIM without controller

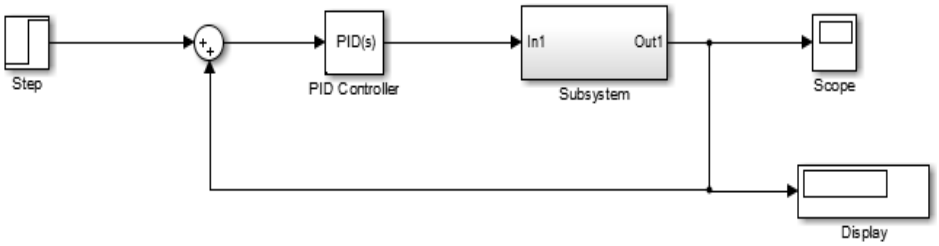

Figure 5. Simulink model with PID controller

5. NEURAL NETWORK CONTROLLER

In the recent years, ANN controllers has given performance effectively to improve nonlinear systems. ANN is implemented in many applications such as electric power and there are promising in dentification/control system, the self-adapting and notable-rapid computing functions of ANN cause them to well desirable to deal with nonlinearities [25, 26].This model consists of two nets, the first net implement is a controller and the other net simulates a version of the plant, NARMA-L2 model can be used to model the plant previously cited, using two distinct neural networks, it makes use of a nonlinear identification tool. The neuro controller is noted by special names: nonlinear auto-regressive moving average and feedback linearization control, while the plant model has a selected method (associate formulation), the plant model can be estimated by NARMA-l2 controller when the same formula, therefore the object of NARMA-L2 is to convert the system from nonlinear to linear dynamics system [27], when using the NARMA-L2 controller, the first step is identify the plant model, that is included of two functions f and g [28], these functions are representing the past values for each the output (y) and the control effort (u) determine by tapped delay lines (TDL), while the second step includes simply the rearrangement ofthe two sub networks f and g trained offline, at the result the computation time is decrease [29]. Figure 6 can be shown NARMA-L2 control structure, when using the NARMA-L2 controller, the first step is identify the plant model, that is included of two functions f and g [28], these functions are representing the past values for each the output (y) and the control effort (u) determine by tapped delay lines (TDL), while the second step includes simply the rearrangement of the two sub networks f and g trained offline, at the result the computation time is decrease [29]. Figure 7 shows the model which consists of WRIM with NARMA-L2 controller that includes two input and one output represents starting torque. This model consists of multi hidden layers variation with the value of external resistance.

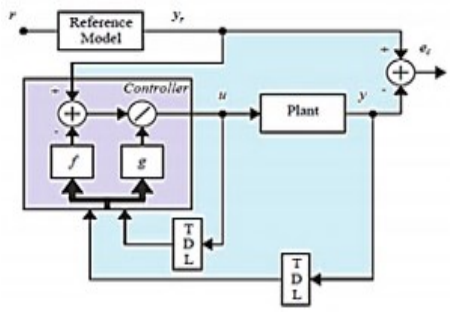

Figure 6. NARMA-L2 control structure

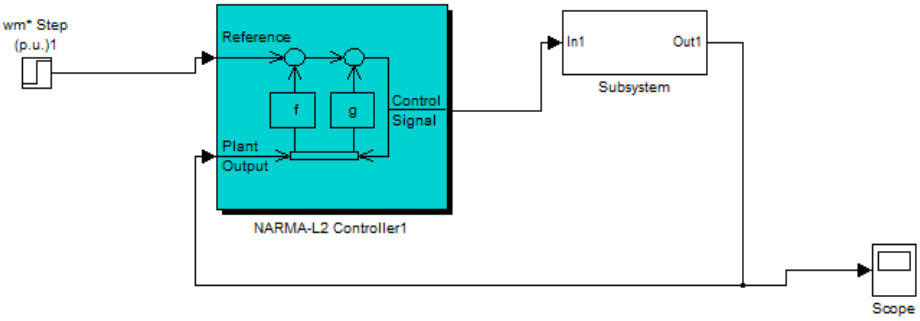

Figure 7. The model of WRIM with NARMA-L2

6. SIMULATION RESULT AND DISCUSSIONS

This part of paper discuss simulation results of WRIM using MATHLAB SIMULINK environment which achieves real-time observation to obtain best torque at starting by adding (R_{ext}) to rotor circuit with values 0.05Ω, 0.1Ω and 0.15Ω because this resistance led to decrease starting current and therefore (T_s) increase but up of this value of R_{ext} the current began to increase and T_s decrease, also this paper use two different control techniques such as conventional controller (PID) controller as well as intelligent controller (ANN (NARMA-L2)) to improve T_s of motor that led to develop the performance of the motor. The parameters of WRIM considered in this paper are summarized in the Table 1.

Table 1. Parameters of WRIM

Parameters	Spesification
Phase	3-Phase
Frequency	50 HZ
Power	2.2 KW/3HP
Pole	6
Efficency %	81%
Speed	1000RPM
Voltage of stator	415 V
Winding	Y-connection
Stator resistance	0.7384 Ω
Stator inductance	3 mH
Rotor resistance	0.7402 Ω
Rotor inductance	3 Mh
Mutual inductance	0.1241 H
Torque	14.85 N-m
Rotor Inertia	0.0343 Kg-m^2

6.1. Simulation result with R_{ext} only

This part of simulation results shows using external resistance adding to rotor circuit (star- connecting) by using MathLab/simulink model in order to increase T_s of motor which leads to better performance, this part takes three values of external resistance which are R_{ext} (0.05Ω, 0.1Ω and 0.15 Ω), in this case starting torque values increase with adding external resistance and equal to (722N.m, 1140N.m, and 1232 N.m) respectively, Figure 8 shows simulation results of model without any controller also Table 2 indicate the values of T_s at these different values of R_{ext}.

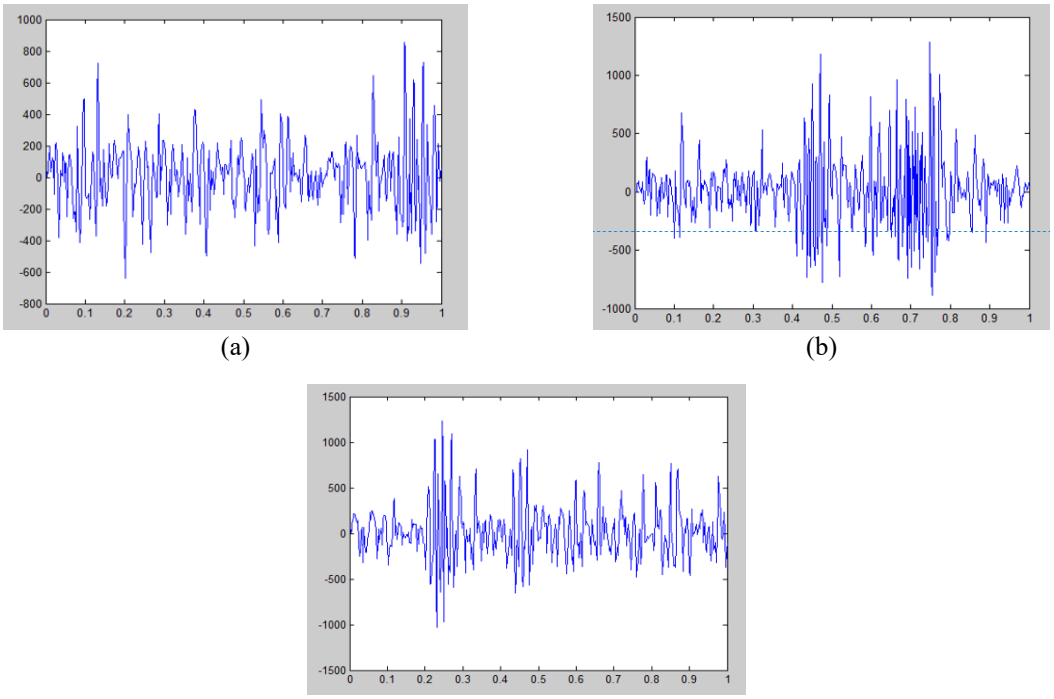

Figure 8. Simulation result without controller; (a) T_s at R_{ext} = 0.05 Ω, (b) T_s at R_{ext} = 0.1 Ω, (c) T_s at R_{ext} = 0.15 Ω

Table 2. Simulation result without controller

Rext (Ω)	T_s (N.m)
0.05	722
0.1	1140
0.15	1232

6.2. Simulation results by using PID controller

This part of paper deals with using PID controller to improve (T_s) than the first case above, by using this controller T_s increase to 1754 N-m When R_{ext} = 0.05 Ω while the values of constant gains of PID controller which represented in proportional gain (K_P=3), integral gain (K_i = 1) and derivative gain (K_d = 0.001) also the value of T_s equal to 1840N.m when R_{ext} = 0.1 Ω and 2080N.m at R_{ext} = 0.15 Ω, Figure 9 shows these results by using PID controller. Table 3 indicates to the values of constant gains for PID controller and T_s for each value of R_{ext}.

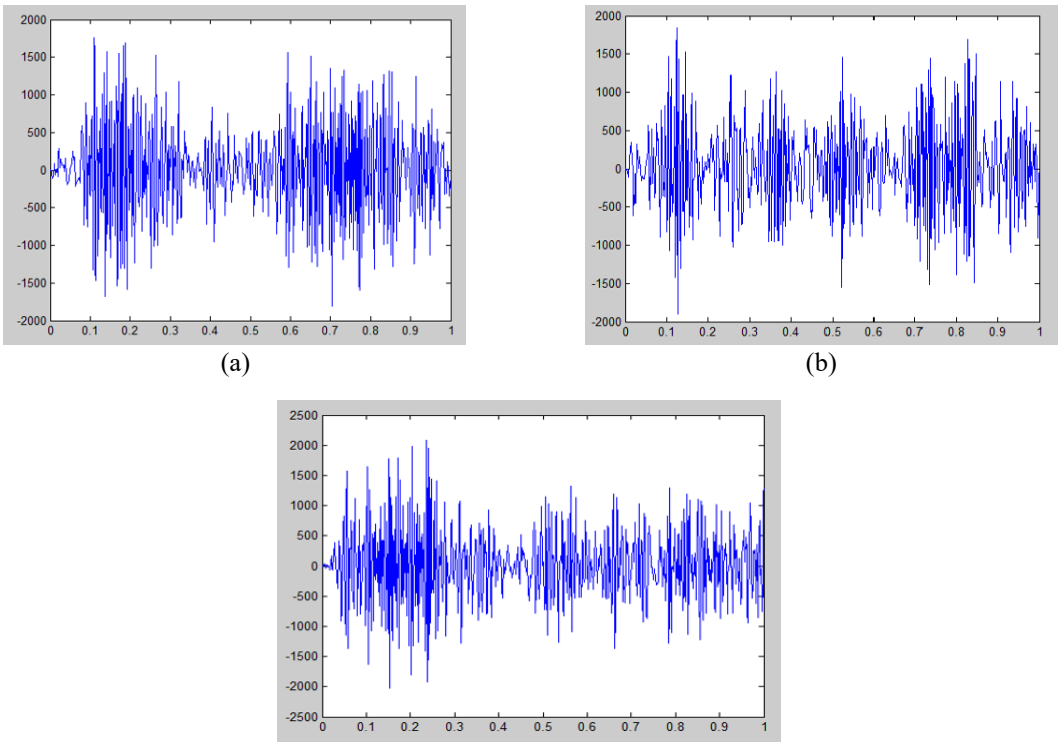

Figure 9. Simulation results with PID controller, (a) T_s at R_{ext} = 0.05 Ω, (b) T_s at R_{ext} = 0.1 Ω, (c) T_s at R_{ext} = 0.15 Ω

Table 3. Constant gains of PID and T_s

R_{ext} (Ω)	Gains of PID	Ts (N.m)
0.05	K_P=3, K_i=1, K_d=0.001	1754
0.1	K_P=5, K_i=1, K_d=0.001	1840
0.15	K_P=3, K_i=2, K_d=0.001	2080

6.3. Simulation result by using NARMA-L2

This part of paper discuss using artificial neural network (NARMA-L2), this intellegrnt technique achieves improving T_s than two other previous cases by obtaining higher T_s in order to develop performance of WRIM, this network is controlled by network architecture which represented by number of delayed plant input, number of delayed plant output and size of hidden layers, in addition to training data to get simulation results. Also this part consists of three states include three different values of R_{ext} (0.05Ω, 0.1Ω and 0.15 Ω) and NARAMA-L2 is trained at each external resistance value to obtain highest starting torque.

6.3.1. Simulation result at R_{ext} = 0.05 Ω

This part refers to simulation results of the model by using NARMA-L2, the value of starting torque which equal to 1940 N.m and number of delayed plant input and output of NARMA-L2 that equal to 4 and 3 respectively while size of hidden layers = 13, sampling interval = 0.001, training samples = 3000, maximum plant input = 4, minimum plant input = -1, minimum plant output = 0.2, maximum interval value =1, minimum interval value = 0.1, Figure 10 shows these simulation results include neural network, plant identification-NARMA-L2 in (a), (b) while (c) indicate to T_s, as well as (d), (e), and (f) show each of training, testing and validation data for NARMA-L2, wheras (g), (h), and (i) show neural network training for each performance, state and regression.

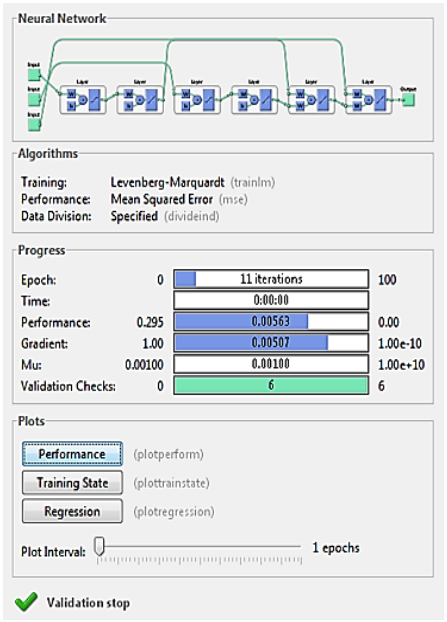

(a)

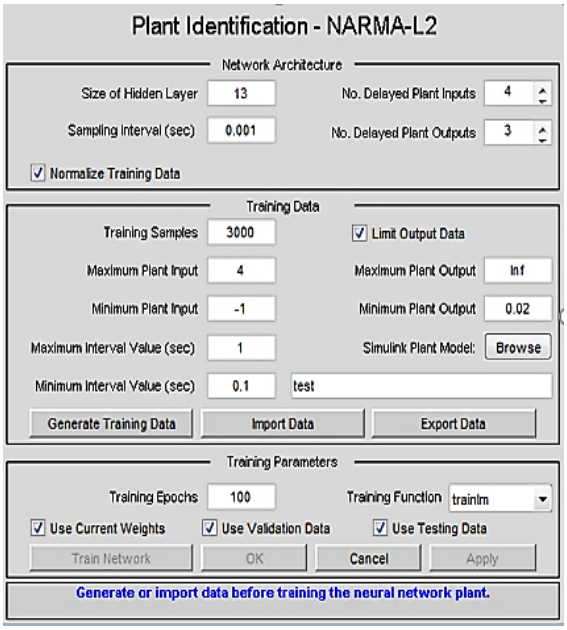

(b)

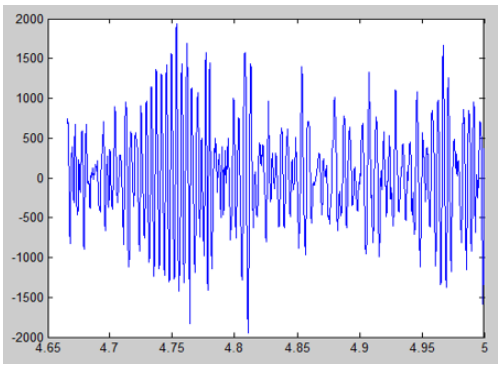

(c)

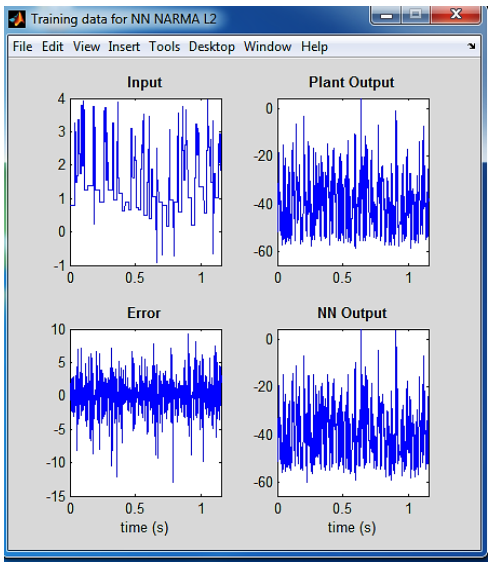

(d)

Figure 10. Simulation results by using NARMA-L2 at R ext = 0.05 Ω; (a) neural network, (b) plant identification-NARMA-L2, (c) Ts = 1940 N.m, (d) training data

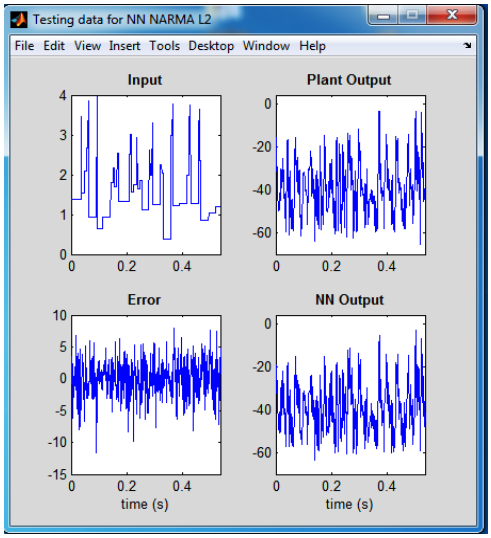

(e)

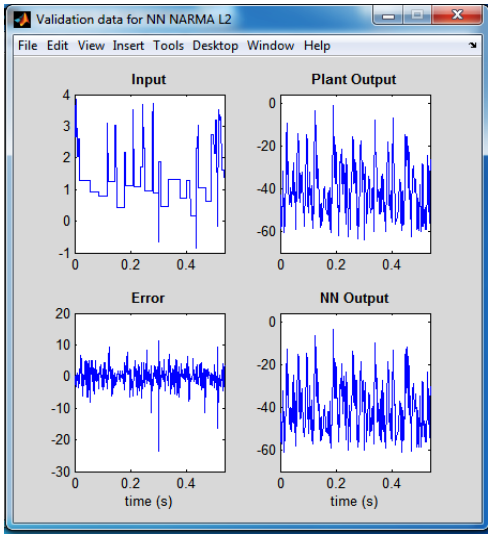

(f)

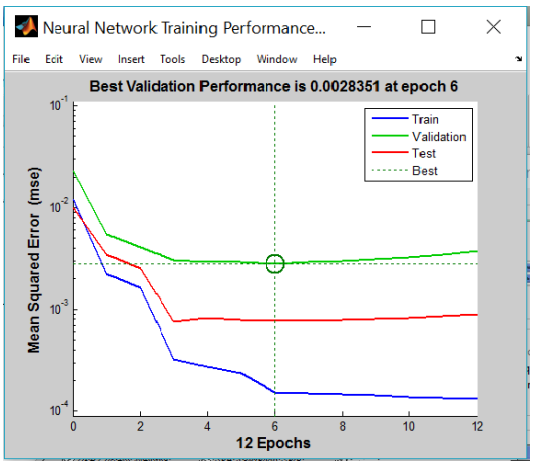

(g)

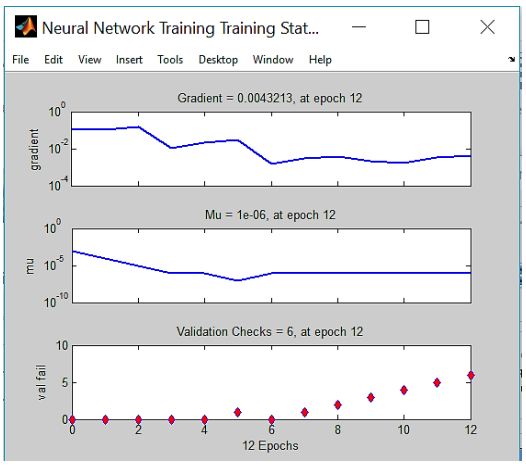

(h)

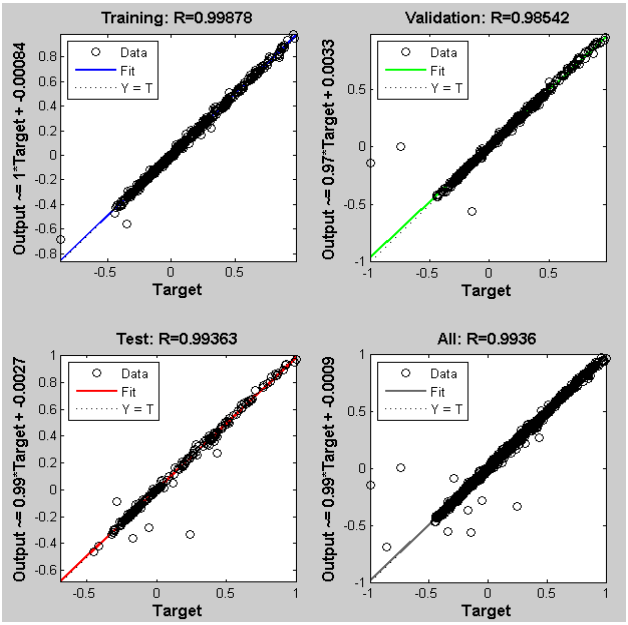

(i)

Figure 10. Simulation results by using NARMA-L2 at R_{ext} = 0.05 Ω; (e) testing data, (f) validation data, (g) training performance, (h) training state, (i) training regression (continue)

6.3.2. Simulation results at R_{ext} = 0.1 Ω

In this part simulation results show when R_{ext} increases to 0.1 Ω and by training NARMA-L2, we get higher starting torque compared to previous case when R_{ext} = 0.05 Ω and the value of starting torque reaches 2150 N.m, Figure 11 shows simulation result of model, (a) refers to plant identification-NARMA-L2 with number of both delayed plant input and output of NARMA-L2 which equal to 2,3 respectively, whereas size of hidden layers = 8, (b) shows the value of T_s, also (c), (d), (e) refer to data for NARMA-L2, as well as (f), (g), and (h) show network training neural for each performance, state and regression.

6.3.3. Simulation results at R_{ext} = 0.15 Ω

Figure 12 refers to simulation results which indicate to increase T_s to 2200N.m and number of delayed plant input and output = 4.3 respectively while size of hidden layer = 9, in this part we obtain higher and best value of T_s than two other cases. Table 4 shows all simulation results by using NARMA-L2 include T_s, number of delayed plant input and output as well as size of hidden layer for each case. Table 5 shows the comparison of simulation results by using (R_{ext}) adding to rotor circuit of WRIM at three cases without controller and with two techniques include conventional PID controller and artificial neural network (NARMA-L2), these results indicate to NARMA-L2 controller gives higher value of T_s than two other cases under the same value of R_{ext}. From above we conclude one of the ways to increase T_s in WRIM is adding R_{ext} to rotor circuit by decrease stating current in order to improve the performance of the motor.

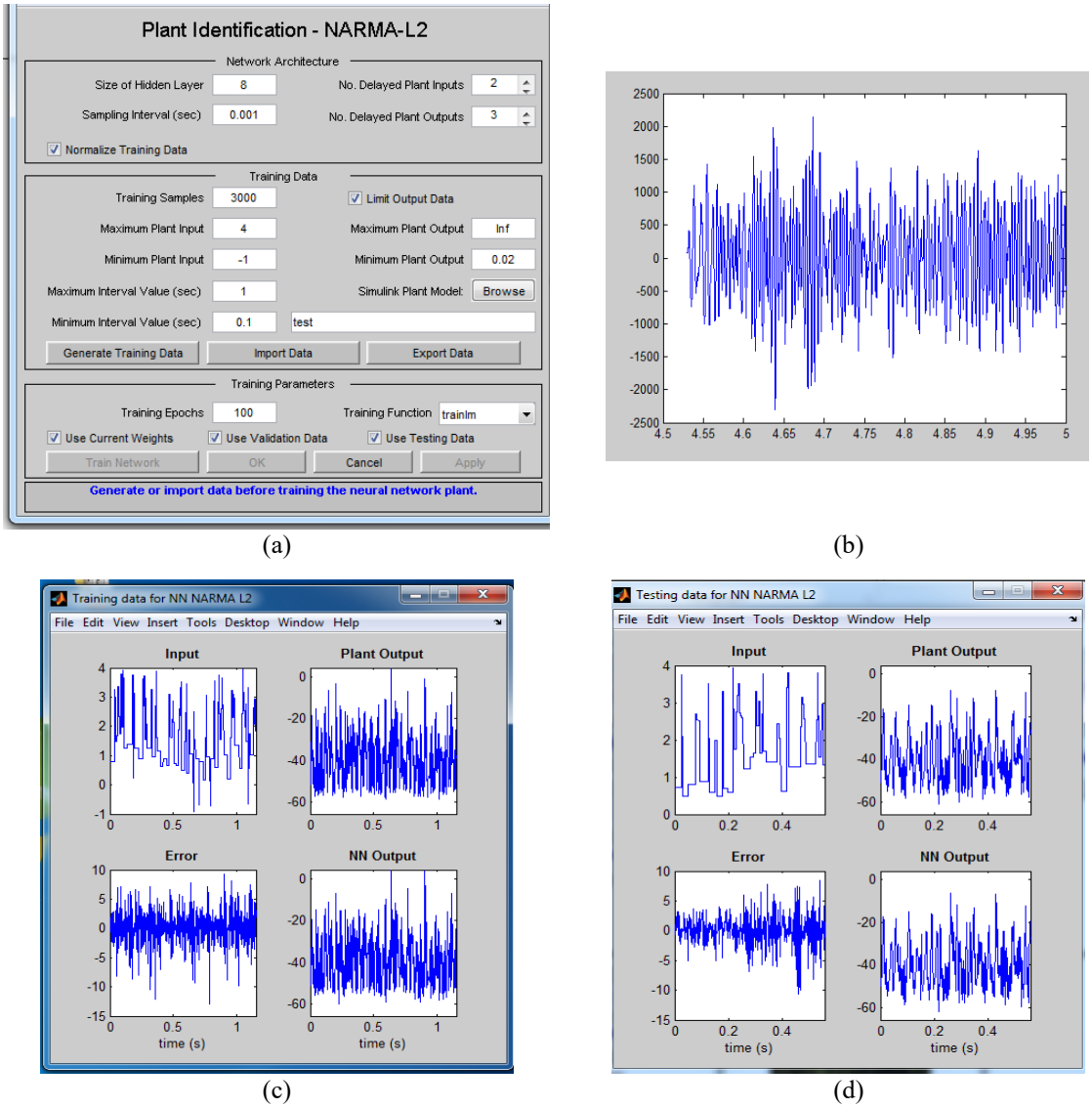

Figure 11. Simulation results by using NARMA-L2 at Rext = 0.1 Ω; (a) plant of NARMA, (b) Ts = 1940 N.m, (c) training data, (d) testing data

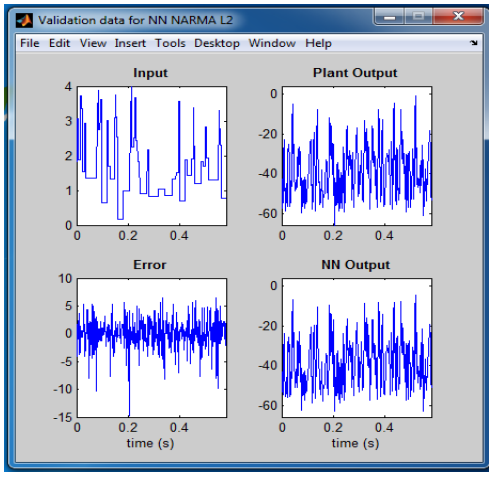

(e)

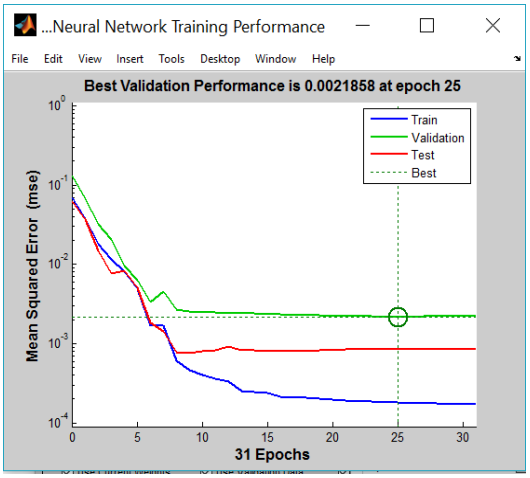

(f)

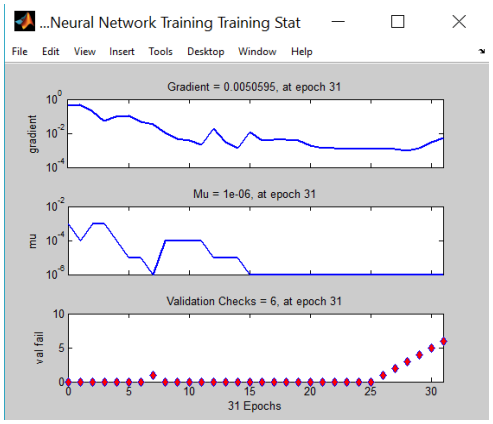

(g)

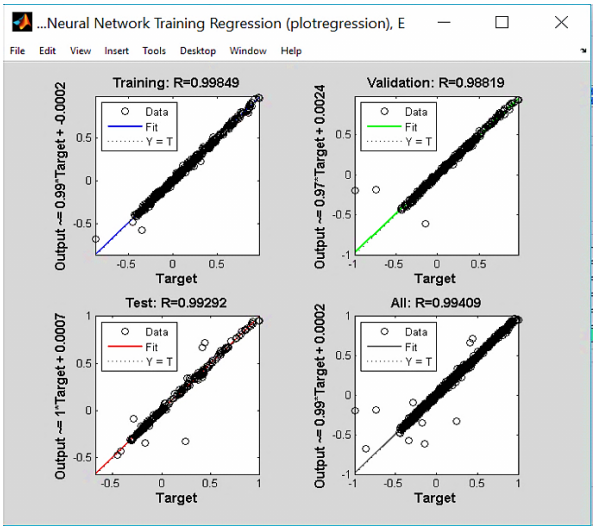

(h)

Figure 11. Simulation results by using NARMA-L2 at R_{ext} = 0.1 Ω; (e) validation data, (f) training performance, (g) training state, (h) training regression (continue)

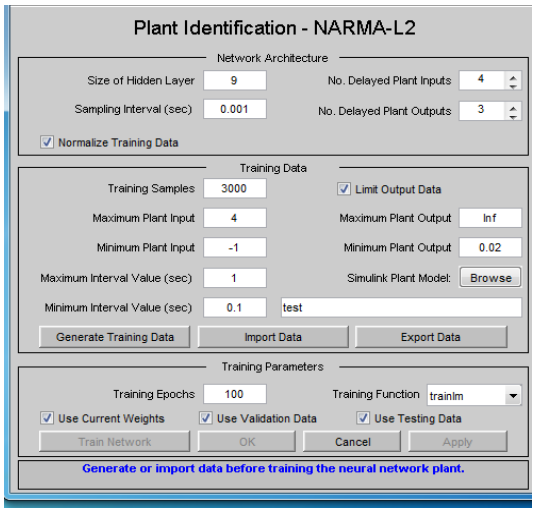

(a)

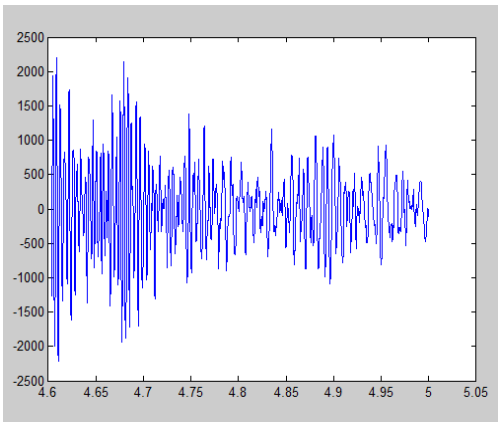

(b)

Figure 12. Simulation results by using NARMA-L2 at R_{ext} = 0.15 Ω; (a) plant of NARMA, (b) T_s = 2150 N.m

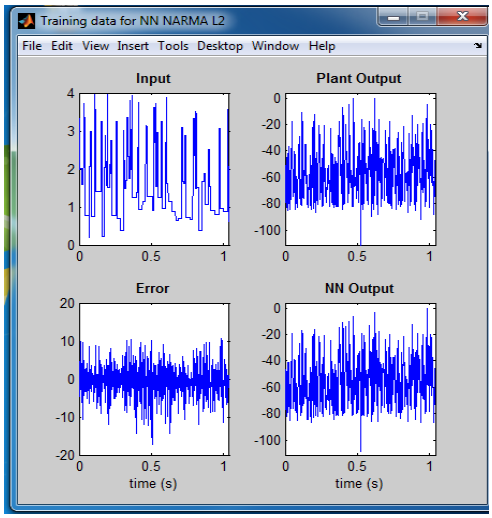

(c)

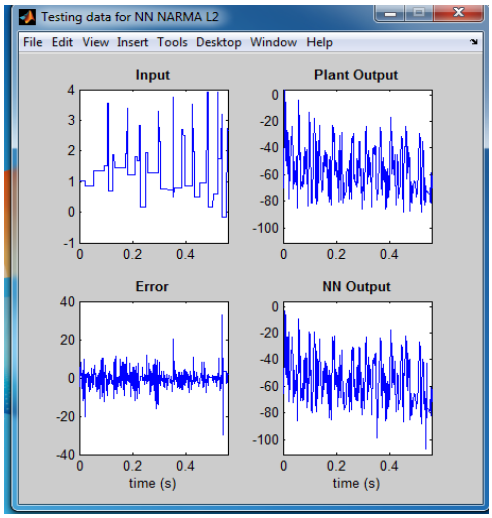

(d)

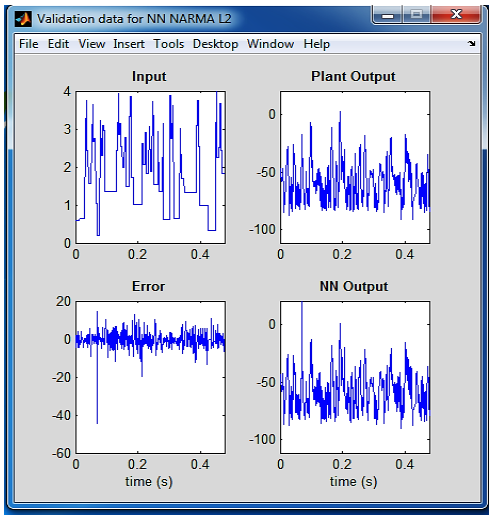

(e)

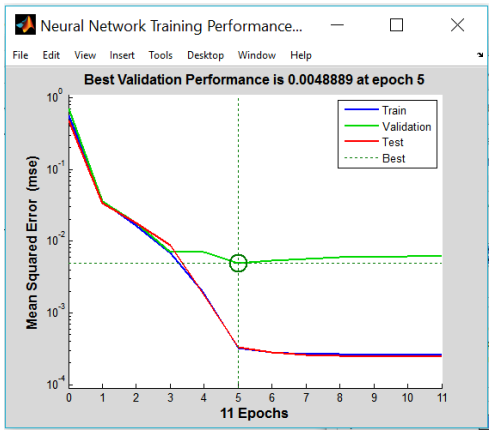

(f)

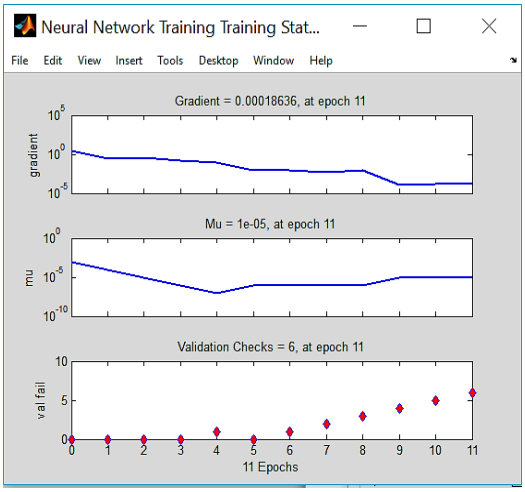

(g)

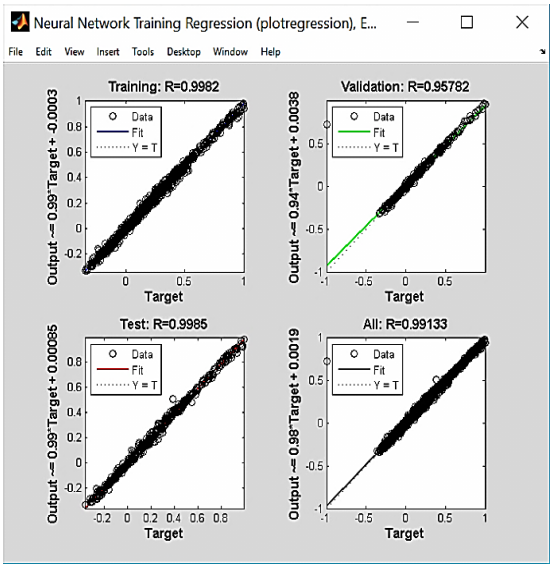

(h)

Figure 12. Simulation results by using NARMA-L2 at $R_{ex\,t} = 0.15\ \Omega$; (c) training data, (d) testing data (e) validation data, (f) training performance, (g) training state, (h) training regression (continue)

Table 4. Simulation results with NARMA-L2

R_{ext} (Ω)	Parameters of NARMA-L2 plant	T_s (N.m)
0.05	I/P = 4, O/P = 3 Hidden layers = 13	1940
0.1	I/P = 2, O/P = 3 Hidden layers = 8	2150
0.15	I/P = 4, O/P = 3 Hidden layers = 9,	2200

Table 5. Comparison simulation results

R_{ext}(Ω)	T_S (N.m) without controller	T_s (N.m) by using PID	T_s (N.m) by using NARMA-L2
0.05	722	1754	1940
0.1	1140	1840	2150
0.15	1232	2080	2200

7. CONCLUSION

This paper proposes adding external resistance to the rotor circuit of 3-phase wound rotor induction motor with three different values (0.05 Ω, 0.1 Ω, 0.15 Ω), this model uses conventional PID controller and artificial neural netwok (NARMA-L2) and training this network to obtain the best starting torque at each value of external resistance. A comparative study between PID controller and (NARMA-L2) has presented to develop performance of the motor at starting. The simulation results has demonstrated a successful implementation of adaptive neural network (NARMA-L2) which gives better results than PID controller by obtaining a highest starting torque and achive improving performance of WRIM.

REFERENCES

[1] K. Ranjith Kumar, S. Palaniswami and G. Lourds Shiny, "Performance enhancement of wound rotor induction motor by rotor capacitive reactance control using fuzzy controller," *International Journal of Electrical Engineering*. vol. 3, no.9, pp.197-207, July 2012.

[2] S. Chandran, "Rotor resistance adaptation scheme using neural learning algorithm for fuzzy logic based sensor less vector control of induction motor," *IOSR Journal of Electrical and Electronics Engineering*, vol. 8, no. 1, pp. 13-21, 2013.

[3] Hanan Mikhael D., *et al.*, "Speed control of induction motor using PI and V/F scalar vector controllers," *International Journal of Computer Applications*, vol. 151, no.7, pp. 36-43, October 2016.

[4] Z. Li, *et al.*, "Rotor speed and stator resistance identification scheme for senseless induction motor drive," *TELKOMNIKA Telecommunication Computing Electronics and Control*, vol 11, no.1, pp. 503-512, 2013.

[5] C. T. Pham, A. W. Shen, "A comparative study of control methods for induction motor and high performance Z-source inverter," *TELKOMNIKA Telecommunication Computing Electronics and Control*, vol 11, no.6, pp. 2912-2925, June 2013.

[6] V. V. Maruti Prasad, W. Prasanna Narasimham, G Sai Raghu Ram, "Rotor Side control of high power slip ring induction motor using single thyristor," *IOSR Journal of Electrical and Electronics Engineering*, vol.9, no. 2, pp. 49-53, March-April 2014.

[7] M. B. Bannae Sharifian, *et al*., "A new soft starting method for wound-rotor induction motor," *Journal of Electrical Engineering*, vol.62, no.1, pp.31-36, January 2011.

[8] R. M. Hamouda, A. I. Alolah, M. A. Bader and M. A. Abdel-Halim, "A Comparative Study on the Starting Methods of Three Phase Wound-Rotor Induction Motors," *IEEE Transactions on Energy Conversion*, vol.14, no. 4, December 1999.

[9] D. D. Dhawale, *et al*., "Analysis of different starting methods of induction motor," *IJARIIE*, vol.3, no. 2, pp. 2484-2494, 2017.

[10] S. AL-Jufout, Kamal Khandakji, "Dynamic simulation of starting and chopper speed control of wound-rotor induction motor," *International Journal of Simulation Systems Science & Technology*, vol. 8, no 2, July 2007.

[11] B. M. Frederic, *et al.*,"The control of induction electromotor by the resistance change in rotor circuit," *American Journal of Engineering Research (AJER)*, vol.8, no. 7, pp-169-175, 2019.

[12] R. Essakiraj, *et al*., "Speed control of induction machine using GA based PID controller*," Middle- East Journal of Scientific Research 23(Sensing, Signal Processing and Secuirty)*, pp.164-169, 2015.

[13] M. George, K. P. Basu, "NARMA-L2 controlled variable frequency three-phase induction motor drive," *European Journal of Scientific Research*, vol. 70, no. 1, pp. 98-111, February 2012.

[14] H. Sh. Dakheel, "Speed control of separately DC motor using artificial neural network," *ournal of Engineering and Development*, Vol.16, No.4, pp.349-362, Dec. 2012.

[15] R. Kumar, R. Dogra and P. Aggarwal, "Rotor side speed control methods using MATLAB/Simulink for wound induction motor," *International Journal of Mechanical and Mechatronics Engineering*, vol.11, no. 7, pp. 1378-1386, 2017.

[16] M. A. Abdel-Halim, *et al.*, "Smooth starting of slip ring induction motors," *IEEE Transactions on Energy Conversion*, Vol.12, No.4, December 1997.

[17] C. Sooji, *et al*., "MATHLAB/simulink based design and simulation of speed control of three phase slip ring induction motor using chopper," *International Journal of science, Engineering and Technology Research (IJSETR)*, vol. 5, no. 1, pp.267-274, January 2016.
[18] K. Devi, S. Gautam and D. Nagaria, "Speed control of 3-phase induction motor using self tuning fuzzy PID controller and conventional PID controller," *International Journal of Information and Computation Technology*, vol.4, no.12, pp.1185-1193, 2014.
[19] S. W. Shneen, *et al*., "Biogeography based optimization tuned fuzzy logic controller to adjust speed of electric vehicle," *Indonesian Journal of Electrical Engineering and ComputerScience (IJEECS)*, vol.16, no. 3, pp. 509-519, December 2015.
[20] M. L. Mhaisgawali and S. P. Muley, "Speed control of induction motor using PI and PID controller," *IOSR Journal of Engineering (IOSRJEN)*, vol.3, no. 5, pp25-30, May 2013.
[21] M. M. Abdullah Alqadasi, *et al*., "Optimization of PID for industrial electro-hydraulic actuator using PSOGSA," *TELKOMNIKA Telecommunication Computing Electronics and Control*, vol.17, no.5, pp. 2625-2635. October 2019.
[22] A. J. Attiya, *et al*., "Compared with PI, Fuzzy _PI & PSO_PI controllers of robotic grinding force servo system," *TELKOMNIKA Telecommunication Computing Electronics and Control*, vol.16, no.1, pp. 65-74, October 2015.
[23] A. Budianto, *et al.,* "PID control design for biofuel furnace using Arduino," *TELKOMNIKA Telecommunication Computing Electronics and Control*, vol. 18, no.6, pp.3016-3023, December 2018.
[24] B. Ahmed Obaid, *et al.,* "Resolving of optimal fractional PID controller for DC motor drive based on anti-windup by invasive weed optimization technique," *Indonesian Journal of Electrical Engineering and Computer Science*, vol. 15, no.1, pp. 95-103, July 2019.
[25] S. W. Shneen and Chengxiong Mao, "Artificial optimal fuzzy control strategy for elevator drive system by using permanent magnet synchronous motor," *TELKOMNIKA Telecommunication Computing Electronics and Control*, vol.14, no.3, pp. 470- 480, June 2015.
[26] S. Arun Balaji and K. Baskaran, "Design and development of artificial neural networking (ANN) system using sigmoid activation function to predict annual rice production in tamilnadu," *International Journal of Computer Science, Engineering and Information Technology (IJCSEIT)*, vol.3, no.1, February 2013.
[27] Abdulrahim T. Humod, *et al.,* "Direct torque control for permanent magnet synchronous," *Eng. &Tech. Journal*, vol. 34, no.3, pp.464-482, 2016.
[28] I. Iulia and A. Mihail, "Design of NARMA-L2 neural controller for an induction motors speed control," *Journal of Computer Science and Control Systems*, vol.6, no.2, pp. 18-21, October 2013.
[29] K. Srakaew, *et al*., "Design of NARMA-L2 neurocontroller for nonlinear dynamical system," *29th International Conference on Modeling Identification, and Control*, pp. 210-215, February 2010.